

On inverting gravity changes with the harmonic inversion method: Teide (Tenerife) case study

Vladimír POHÁNKA, Peter VAJDA, Jaroslava PÁNISOVÁ

Division of Geophysics, Earth Science Institute, Slovak Academy of Sciences,
Dúbravská cesta 9, 845 28 Bratislava; e-mail: Peter.Vajda@savba.sk

Abstract: Here we investigate the applicability of the harmonic inversion method to time-lapse gravity changes observed in volcanic areas. We carry out our study on gravity changes occurred over the period of 2004–2005 during the unrest of the Central Volcanic Complex on Tenerife, Canary Islands. The harmonic inversion method is unique in that it calculates the solution of the form of compact homogeneous source bodies via the mediating 3-harmonic function called quasigravitation. The latter is defined in the whole subsurface domain and it is a linear integral transformation of the surface gravity field. At the beginning the seeds of the future source bodies are introduced: these are quasi-spherical bodies located at the extrema of the quasigravitation (calculated from the input gravity data) and their differential densities are free parameters preselected by the interpreter. In the following automatic iterative process the source bodies change their size and shape according to the local values of quasigravitation (calculated in each iterative step from the residual surface gravity field); the process stops when the residual surface gravity field is sufficiently small. In the case of inverting temporal gravity changes, the source bodies represent the volumetric domains of temporal mass-density changes. The focus of the presented work is to investigate the dependence of the size and shape of the found source bodies on their differential densities. We do not aim here (yet) at interpreting the found solutions in terms of volcanic processes associated with intruding or rejuvenating magma and/or migrating volatiles.

Key words: volcano gravimetry, gravimetric interpretation, microgravity, temporal gravity changes, gravity inversion

1. Introduction

The aim of this paper is to study the applicability of the harmonic inversion method to interpreting temporal gravity changes occurring in restless

or re-activating volcanic areas by investigating the changes of the subsurface density distribution which caused the gravity changes observed on the surface. To meet this objective we use time-lapse gravity changes observed over the period 2004–2005 during the unrest at the Central Volcanic Complex (CVC) of Tenerife. As the relation between the gravity field and the density distribution generating this field is a linear one (the Newton law), the relation of the change of the gravity field and the change of the density distribution is linear as well. Therefore it is possible to use the harmonic inversion method, previously successfully applied to gravity, also to gravity changes by simply replacing in all formulae the density by the temporal density change and the gravity by the temporal gravity change.

For the gravity inversion we use the harmonic inversion method developed by the first author (*Pohánka, 2001, 2003a*). The method is called harmonic because it is based on the very advantageous properties of n -harmonic functions. Unlike the most of forward modeling methods (e.g., *Brimich et al., 1996, 2011; Charco et al., 2002*), which require an interactive modification of the model parameters by the interpreter until a good fit with input data on the earth surface is reached, direct inversion methods, such as the one applied here, calculate the solution directly from the input data and the interpreter specifies only the starting model.

The main difference between the usual inversion methods and the harmonic inversion is in the number of parameters the values of which have to be calculated: in the former case this number is usually small – smaller than the number of the input gravity values (for example, if the solution is sought in the form of a set of polyhedral anomalous bodies, these parameters are the coordinates of vertices of these bodies). On the contrary, by the harmonic inversion the number of unknown parameters is huge – in any case much greater than the number of the input values. This is because the unknown parameters are the density values for each cubic cell into which the calculation domain is divided; the known parameters are the values of the input gravity interpolated onto a regular grid at the surface. The disparity between the numbers of unknown and known parameters is the straightforward consequence of the difference between the 3-dimensional solution (density distribution) and the 2-dimensional input (surface gravity).

As the harmonic inversion method is not yet developed for the case of arbitrary form of the Earth (topographic) surface, we use here the variant

of the method developed for the planar surface (a flat Earth approximation) disregarding the topography. The negligence of topography can be remedied by applying topographic correction to the observed surface gravity data and eventually by downward continuing the data from topographic surface to sea level.

The harmonic inversion has already been applied to gravity data when studying the crustal structure on a regional scale (*Pohánka, 2001, 2003b*). It was used also in microgravimetric interpretation for archeological investigations when searching for unknown buried cavities such as chambers, tombs, crypts (*Pánisová et al., 2013*). Here we apply the method to dealing with gravity signals at the level of several tens of μGals (like in the near surface microgravimetric studies), specifically to the time-lapse gravity changes observed in volcanic areas during unrest or re-activation, while the spatial dimensions of the study domain are in kilometers to tens of kilometers. As will be shown below, the differential densities (volumetric density changes) of the source bodies are to be selected beforehand (apriori) by the interpreter and for any such choice we obtain different final solution. The main focus of this work is to study the variability of the solutions, namely the sizes and shapes of the found anomalous bodies, depending on the selection of the differential densities.

2. Harmonic inversion method

The inverse problem of gravimetry consists in finding the density distribution in the inversion domain (representing the interior of the Earth) from the given gravity data at the boundary of the inversion domain (representing the surface of the Earth).

The inverse problem of gravimetry has infinitely many solutions and thus it is ill-posed: there exist infinitely many density distributions (which are nonzero in the inversion domain) that generate zero gravity field at the boundary of the inversion domain. Therefore it is convenient to ask whether there is some unique solution which is the simplest possible in certain sense. Such a solution can be found if we represent the simplicity as smoothness: this solution is certain n -harmonic function defined in the inverse domain where n is a small positive integer. Recall that n -harmonic function $f(x, y, z)$ satisfies the equation $\Delta^n f(x, y, z) = 0$ (where Δ is the Laplace

operator in the 3-dimensional space with coordinates x, y, z) (Pohánka 2001, 2003a). There is a unique solution which is harmonic (thus $n = 1$); however, such a solution can have its extrema only at the boundary of the inversion domain and thus cannot represent an anomalous body below the surface of Earth. Therefore we shall require that the inversion procedure has to satisfy the extremum preservation condition defined as follows: if the input is the gravity field of a single point mass lying in the inversion domain, then the solution should have its main local extremum exactly at this point. If we add the requirement that the solution has to be expressed as a linear integral transformation of the input gravity field, we can find an unique solution $\rho(x, y, z)$ for $n = 4$; this is called the characteristic density.

Such a solution is fully satisfactory from the purely mathematical point of view; however, it is in no way a realistic solution because it is everywhere very smooth and thus it cannot represent the real anomalous bodies where the density has jumps at their boundaries. On the contrary, solutions which are piecewise constant functions can be considered very well as realistic ones. For any such solution there is a set of subdomains of the inversion domain such that in each of these subdomains the solution is a constant function (these subdomains represent anomalous bodies). The inversion procedure should thus determine the number of such anomalous bodies and for each body its density and shape; the principle of simplicity tells us that the number of the bodies should be as small as possible and the shapes of the bodies should be as simple as possible – this could mean that the boundaries of the bodies have to be maximally smooth. There remains the main question: how to determine the shape of each of these bodies if our only information is the gravity field at the boundary of the inversion domain?

The usual inversion procedures based on least squares methods have the common drawback arising from the simple fact that they try to determine a 3-dimensional solution using directly the 2-dimensional input. On the other hand, the harmonic inversion method is based on the very useful properties of the above described smooth (but unrealistic) solution: it uses this solution as a tool for the determination of the realistic solution in the form of a set of anomalous bodies with constant densities. It can be shown that we even do not need to use the smooth solution of the inverse problem: we can use any function which is sufficiently smooth and which satisfies the above described extremum preservation condition. The current version of

the method uses the 3-harmonic function called quasigravitation which is not a solution of the inverse problem (in contrast to the previously used characteristic density), but it has the property that for the input in the form of a single point source it has its main extremum located exactly at this point source and the value of this extremum is equal to the peak value of the input gravity field.

In our calculation we used the planar surface version of the inversion procedure where the Earth surface is defined by the condition $z = 0$ and the inversion domain is the lower halfspace ($z \leq 0$); the quasigravitation $q(x, y, z)$ is calculated from the surface gravitation $g(x, y)$ (gravity acceleration) by the formula:

$$z \leq 0 : \quad q(x, y, z) = 8 \int_0^\infty \frac{u^2 z^3}{(u^2 + z^2)^{5/2}} \partial_u \bar{g}(x, y, u) du, \quad (1)$$

where

$$\bar{g}(x, y, u) = \frac{1}{2\pi} \int_0^{2\pi} g(x + u \cos \varphi, y + u \sin \varphi) d\varphi, \quad (2)$$

is the mean value of the surface gravitation at the circle with radius u centered at the point (x, y) .

The inversion procedure works as follows: first the starting model is created, and then this model is iteratively changed until the surface gravity field generated by the model describes the input gravity field sufficiently well. The starting model is determined based on the quasigravitation calculated from the input gravity field: for each local extremum of this quasigravitation there is introduced an initial anomalous body with approximately spherical shape (any anomalous body consist of some number of small cubic cells). The position of the center of the body is located at the position of the extremum; the differential density of the body is preselected by the interpreter – the only condition is that it has to have the same sign as the sign of the extremum of quasigravitation. The radius of the initial spherical body is again preselected by the interpreter – here the only condition is that the maximum of the gravity field generated by the initial body should be smaller (in absolute sense) than the extremum of the quasigravitation.

The following automatic iterative procedure does not change the densi-

ties of the anomalous bodies; it changes only the shapes and sizes of the bodies. In other words, it shifts the boundary of each body at each boundary cell inwards or outwards. This is done as follows: in each iterative step, the surface gravity field of the density model (created in the previous iterative step) is calculated and this field is subtracted from the input gravity field producing a residual gravity field. From this residual field it is then calculated the (residual) quasigravitation; on the contrary to the case of the starting model, this needs not to be done in the whole inversion domain, but only at the cells belonging to the boundaries of the anomalous bodies. Then the boundary of each body is shifted at each boundary cell inwards or outwards according to the sign of the residual quasigravitation at this cell: if this sign is the same as the sign of the differential density of this body, the boundary is shifted outwards (increasing the volume of the body), otherwise the boundary is shifted inwards (decreasing the volume of the body). Of course, this does not mean that the cell itself is somehow shifted: the shifting of the boundary means that the density of the corresponding boundary cell is changed from the original value to the value of the neighbouring cell on the other side of the boundary. Thus, there can never happen that some cell acquires the density other than those of the existing cells.

The changing the density of the boundary cells is controlled by a set of parameters which determine the so-called limiting value of quasigravitation: the cell can change its density only if the actual value of the (residual) quasigravitation at this cell is (absolutely) greater than this limiting value. The limiting value is slowly decreasing with each iteration step and (in each step) it is increasing with the depth. These parameters are set by the interpreter at the beginning of the iterative procedure and their correct choice may substantially improve the shape of resulting anomalous bodies (in the sense of greater regularity of their boundaries).

The iteration procedure should run in ideal case until the residual surface gravity field is smaller (in absolute sense) than some given limit; however, actually the procedure runs for some preselected number of iterative steps and the model is saved always after 8 consecutive steps. In this respect it is interesting that in the actual calculations there happens only rarely that the shapes of the anomalous bodies remain unchanged starting from some iteration step (which means that the calculation is in fact finished). In the most cases the shapes of the anomalous bodies change with each iteration

step although the residual surface gravity decreases only very slowly (and in some cases it can even slowly increase). Often it can happen that the boundaries of the anomalous bodies become fuzzy starting from some iterative step; for an incorrect choice of the parameters mentioned above it can happen that the solution starts to oscillate (the bodies grow in one step and shrink in the next one). Therefore the final solution is not taken from the last iterative step, but from the (saved) iterative step with the lowest absolute values of the residual surface gravity.

It has to be noted that in the original version of the harmonic inversion procedure each initial anomalous body consisted from a single cell. This had the disadvantage that the shape of the resulting anomalous bodies was in many cases distorted (prolonged in the direction away from the surface). Such a behaviour is the consequence of the mathematical properties of the n -harmonic functions which cannot be removed by some other choice of the form of quasigravitation. However, this deformation can be practically removed by creating the initial anomalous bodies in the form of sphere if the volume (and thus also the mass) of the sphere is comparable to the volume of the resulting body (note that this volume can be roughly determined from the value of quasigravitation at the corresponding extremum).

The current versions of the harmonic inversion procedure are developed for the inversion domain of the shape of a sphere or a halfspace, with the boundary of the inversion domain (representing the earth surface) as either the surface of a sphere or a plane. This restriction arises from the fact that the calculation of the quasigravitation is relatively simple in these two cases and it becomes very difficult if the boundary of the inversion domain is an arbitrary (albeit smooth) surface.

3. Gravity changes of the 2004/5 Teide (Tenerife) volcanic unrest

The central volcanic complex (CVC) on Tenerife (Fig. 1), Canary Islands, comprised of the Las Cañadas caldera and the twin strato-volcanoes Pico Viejo (PV) and Teide (T), experienced in 2004–2005 a seismo-volcanic unrest. Among other unrest indicators, spatio-temporal gravity changes were observed at the CVC on 14 benchmarks of a rapid reaction network

(Gottsmann *et al.*, 2006). No statistically significant areal surface deformation (either inflation or deflation) was observed accompanying these gravity changes. The observed gravity changes were corrected for tidal and hydrological effects (*ibid*). These point gravity data were taken as input data in our study (depicted by cross marks in Fig. 2). They were interpolated and extrapolated onto a regular grid in the area 60×60 km with the step 200 m (90601 gravity values).

We applied an interpolation method developed by the first author (Pohánka, 2005). This interpolation method belongs to the class of moving average methods. The interpolated value at any given point is calculated using the input values at all measurement points; each of the latter values contributes according to the weight of the measurement point (with respect to the calculation point) which is a strongly decreasing function of the distance of these two points. First a polynomial of the second order is determined (by the least squares method), which approximates best the measurement point values in the neighborhood of the calculation point; then the interpolated value is simply taken as the value of this polynomial at the calculation point (in other words, from the 6 coefficients determining the polynomial, just one is used). This procedure assures the maximal smoothness of the resulting interpolated function. The interpolated gravity changes are shown in Fig. 2.

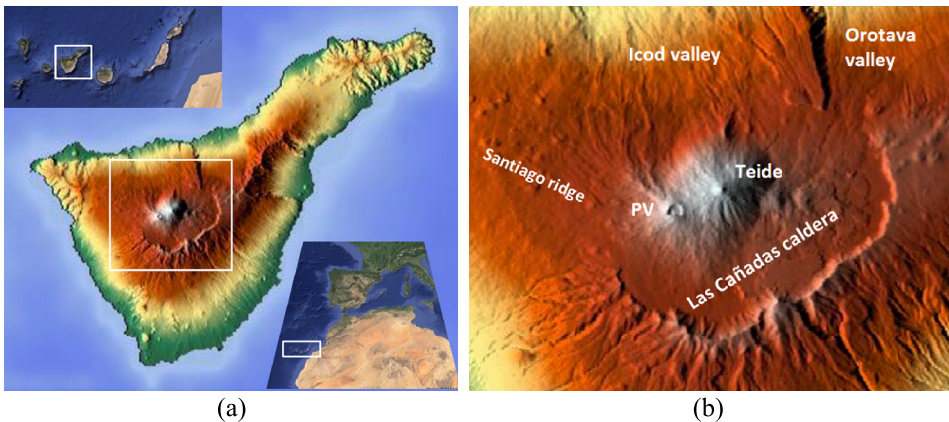


Fig. 1. Location of our test study: (a) Canary islands and Tenerife, (b) the CVC with twin volcanoes.

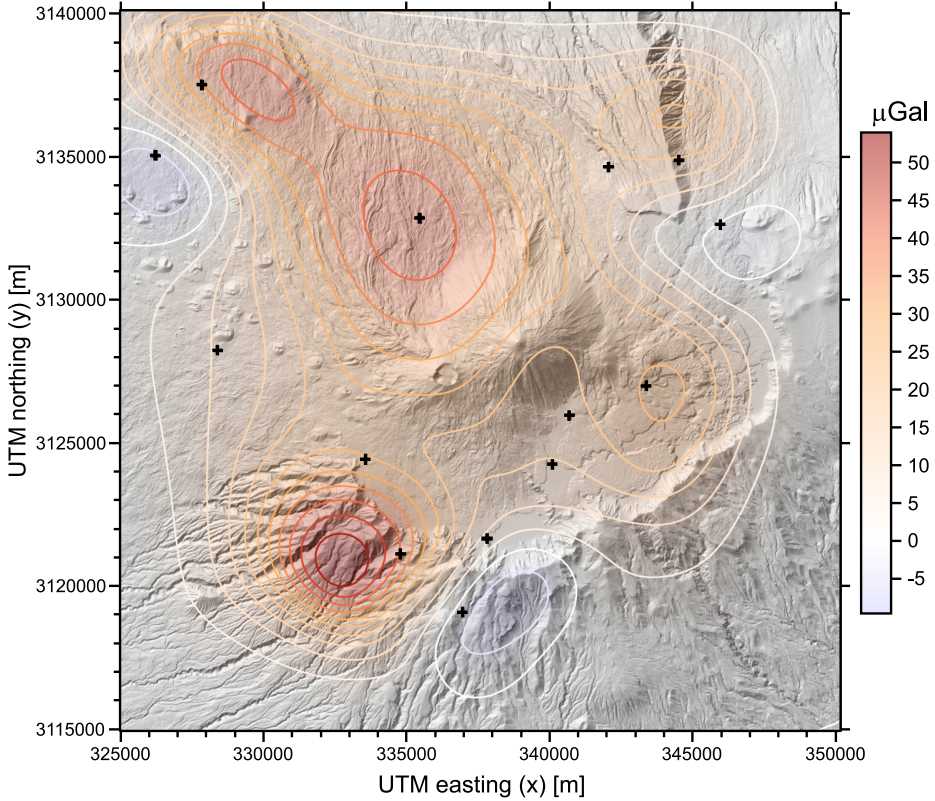


Fig. 2. Temporal gravity changes of the 2004/5 Tenerife unrest interpolated onto a regular grid. The positions of measuring stations are depicted by black cross marks.

4. Harmonic inversion solutions

The quasigravitation for the 2004/5 CVC Tenerife volcanic unrest was computed from the interpolated gravity change values in the rectangular domain with horizontal dimensions 40×40 km and maximum depth 12 km; the step in all dimensions was 200 m (the domain contains 2424060 cubic cells). The result is shown in Fig. 3 in terms of two horizontal sections.

Altogether 11 local extrema of quasigravitation were found: 7 with positive and 4 with negative values. The positions of these local extrema and the corresponding extremal quasigravitation values are listed in Table 1

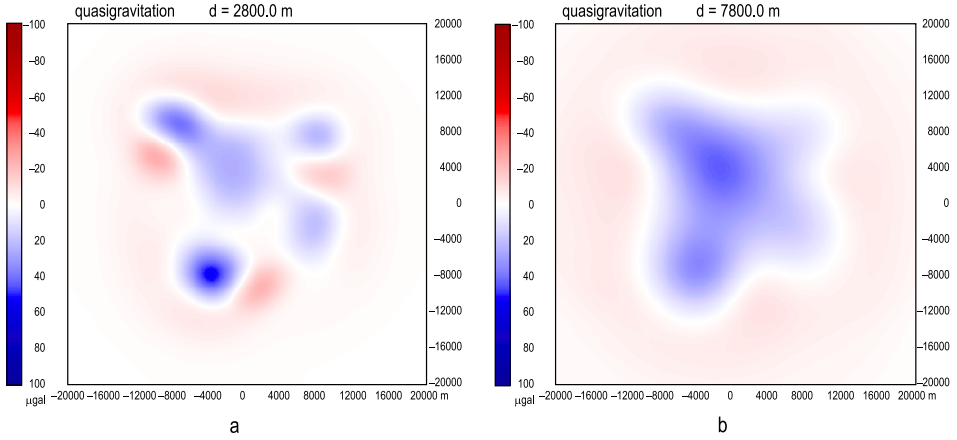


Fig. 3. Quasigravitation: horizontal section at depth of 0.8 km b.s.l. (a) and at depth of 5.8 km b.s.l. (b). Horizontal coordinates are relative to a centre at $x_0 = 336980$ m (UTM easting), $y_0 = 3128520$ m (UTM northing). Blue depicts positive values while red negative values.

Table 1. The local extrema of quasigravitation (as numbered in the first column): x and y are UTM easting and northing, z is height above sea level, q is the value of quasigravitation at the extremum and m^* is the mass equivalent of the quasigravitation extremum (as if the extremum represented a point mass). The last two columns are indicative of the contribution of the extremum to the overall field. For plan view of the locations of the extrema see Fig. 4.

extremum	x (UTM) [m]	y (UTM) [m]	z [m]	m^* [10^9 kg]	q [μ Gal]
1	332980	3120720	-1200	83.208	54.225
2	335180	3132720	-5800	418.300	45.881
3	329180	3137720	-800	45.838	39.016
4	344380	3126120	-1800	52.351	24.193
5	344780	3136320	-600	23.824	23.518
6	331380	3136120	-600	12.211	12.054
7	326780	3138120	+200	5.512	11.352
8	327180	3133920	-1000	-34.371	-25.485
9	338380	3119120	-800	-22.267	-18.953
10	334180	3140920	-4600	-94.114	-14.418
11	345780	3131720	-1000	-18.355	-13.609

and portrayed in Fig. 4. Therefore the starting model consisted of 11 initial anomalous bodies: 7 with the positive and 4 with the negative differential density changes. As for the differential densities attributed to these bodies, there were 7 solution variants considered, with different values of these differential densities, ranging from 1 to 16 kg/m³ for the positive ones and from -1 to -8 kg/m³ for the negative ones. These solutions resulting from the iterative calculation are portrayed in Figs 5 to 11 and their parameters are listed in Tables 2 to 4 (for the solutions from Figs 5, 6 and 11) further below. For simplicity (and clarity of the depictions) the bodies with negative differential density are not shown in Figs 5 to 11.

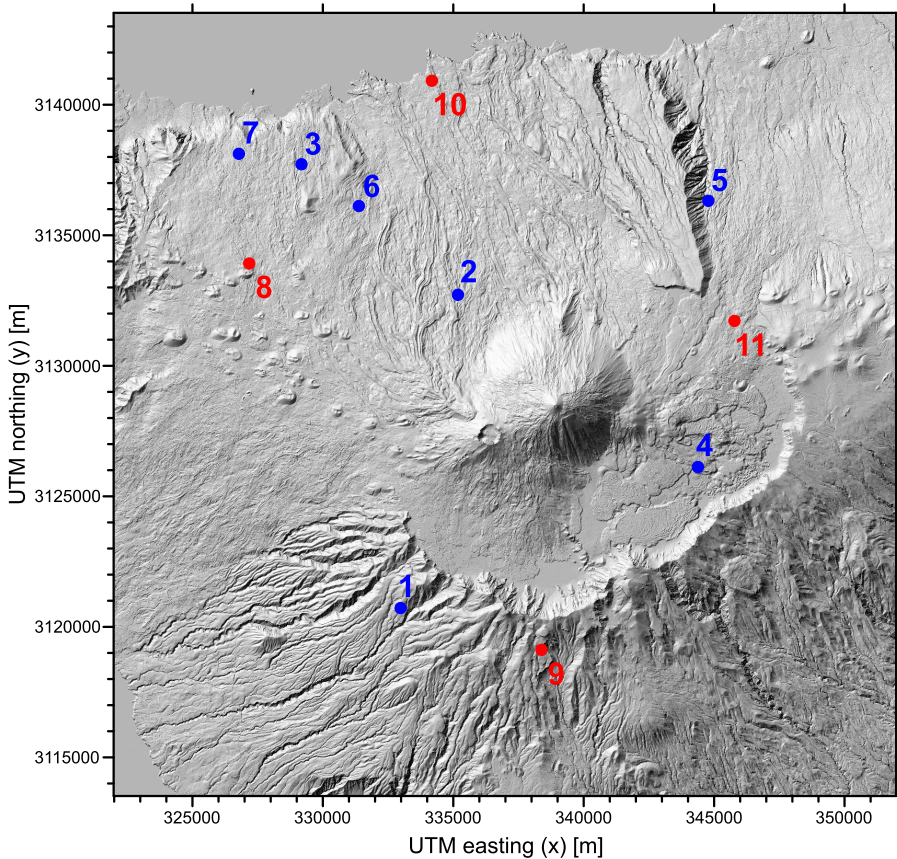


Fig. 4. Plan view of locations of the local extrema of the quasigravitation, see Table 1 for coordinates and values.

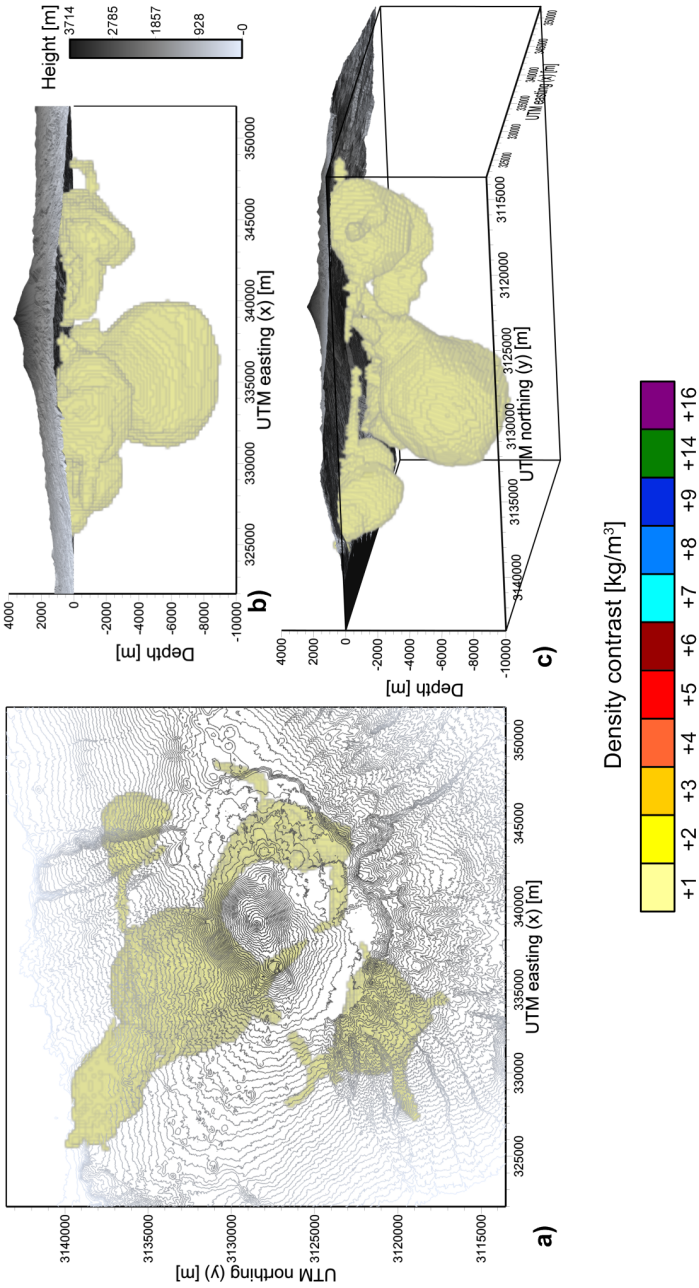


Fig. 5. Solution A. Source bodies with differential densities of +1 kg/m³: (a) plan view, (b) and (c) are two different angle-views.

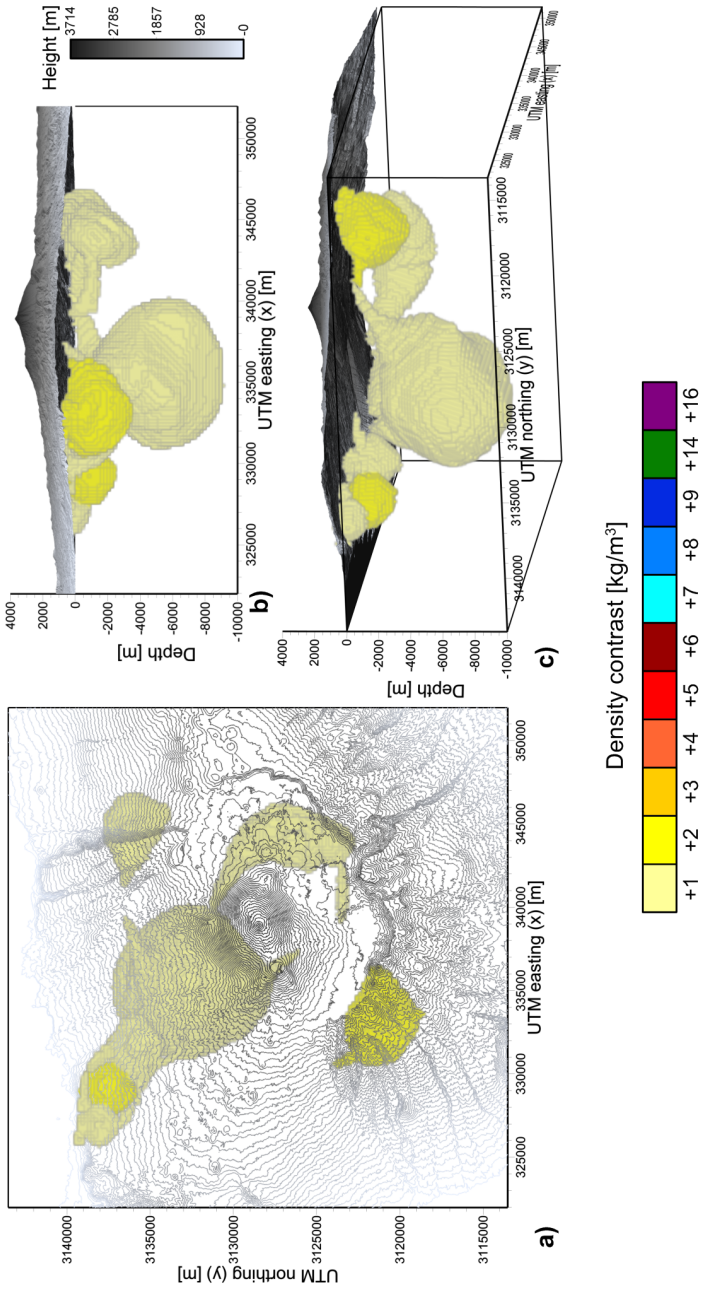


Fig. 6. Solution B. Source bodies with differential densities of +1, and +2 kg/m³: (a) plan view, (b) and (c) are two different angle-views.

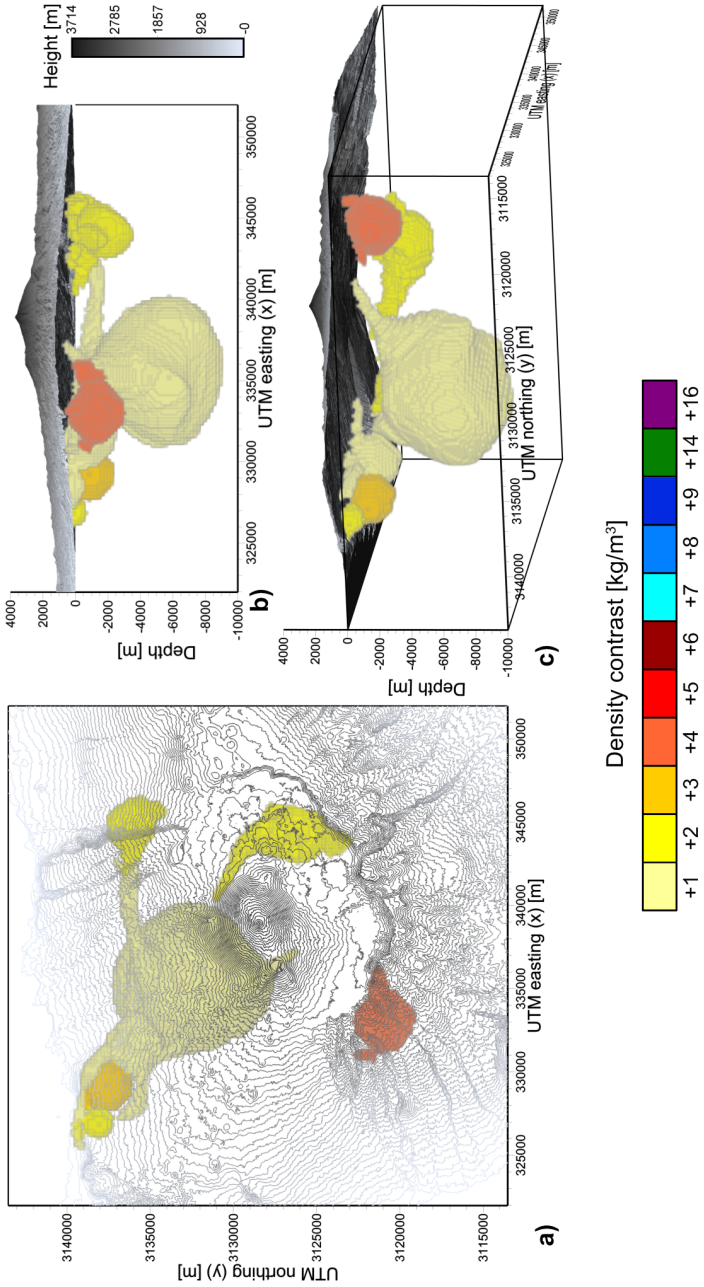


Fig. 7. Solution C. Source bodies with differential densities of +1, +2, +3 and +4 kg/m³; (a) plan view, (b) and (c) are two different angle-views.

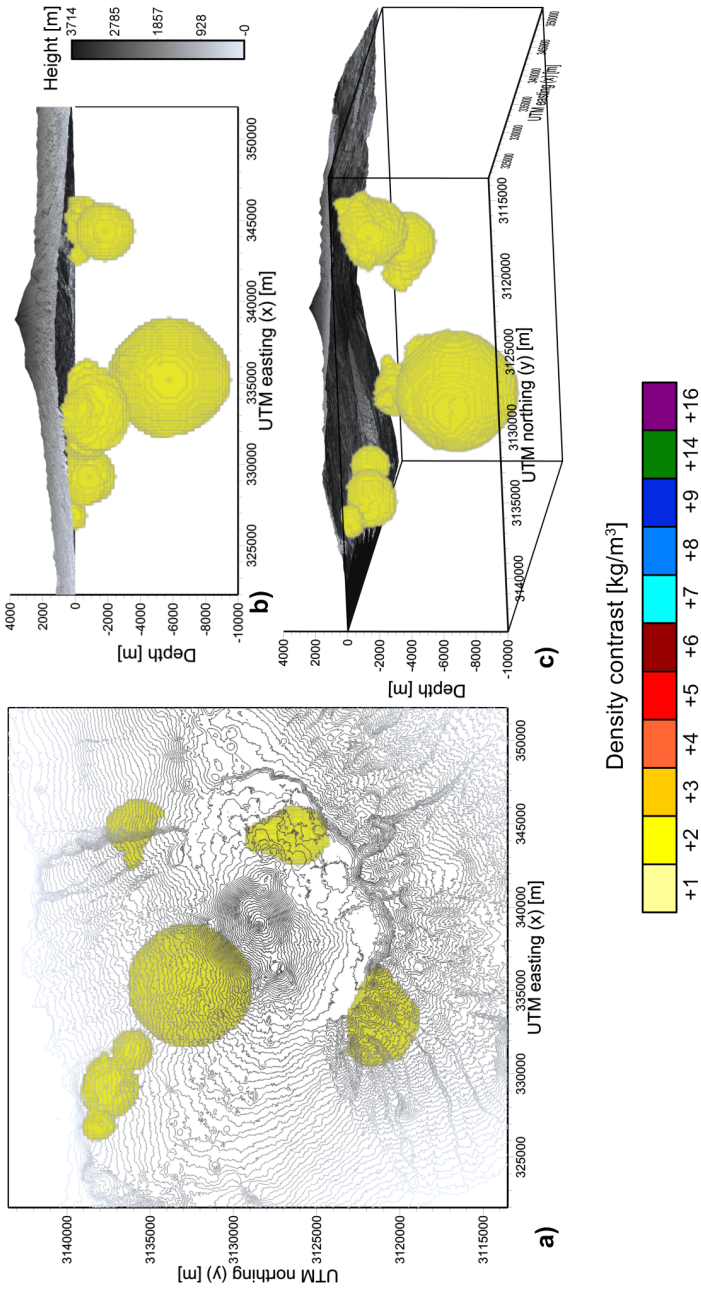


Fig. 8. Solution D. Source bodies with a common differential density of $+2 \text{ kg/m}^3$: (a) plan view, (b) and (c) are two different angle-views.

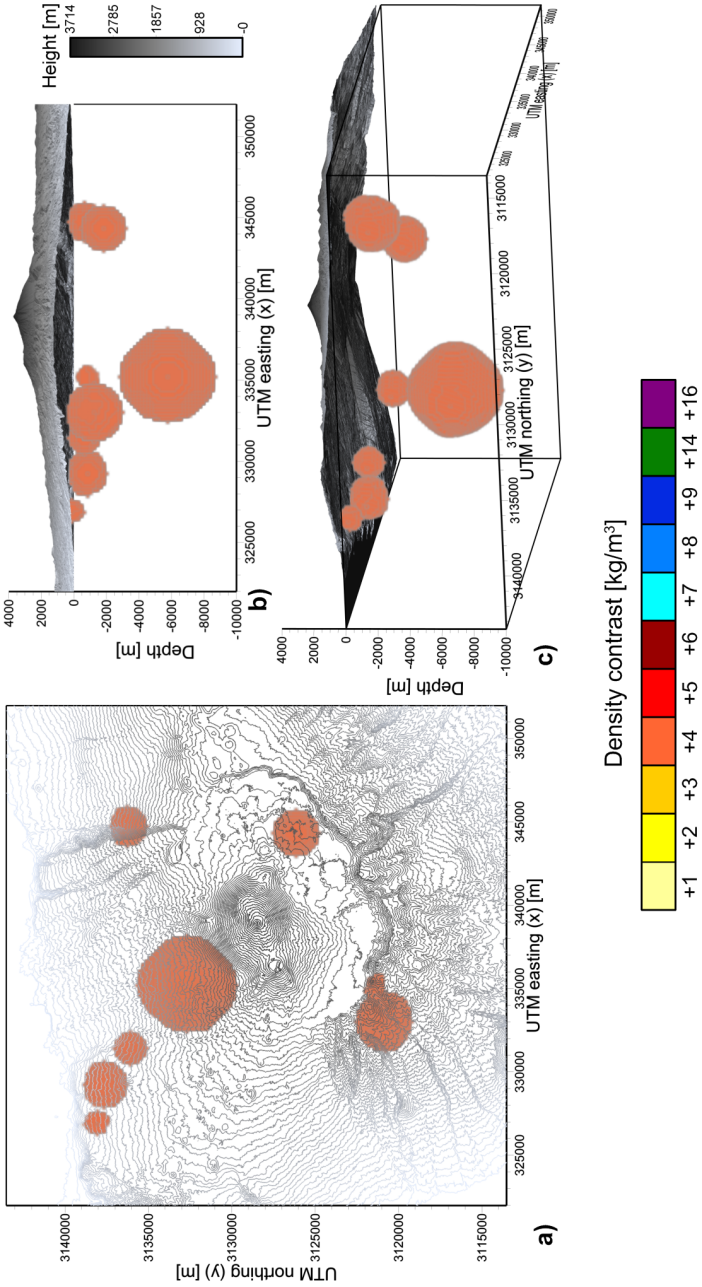


Fig. 9. Solution E. Source bodies with a common differential density of +4 kg/m³: (a) plan view, (b) and (c) are two different angle-views.

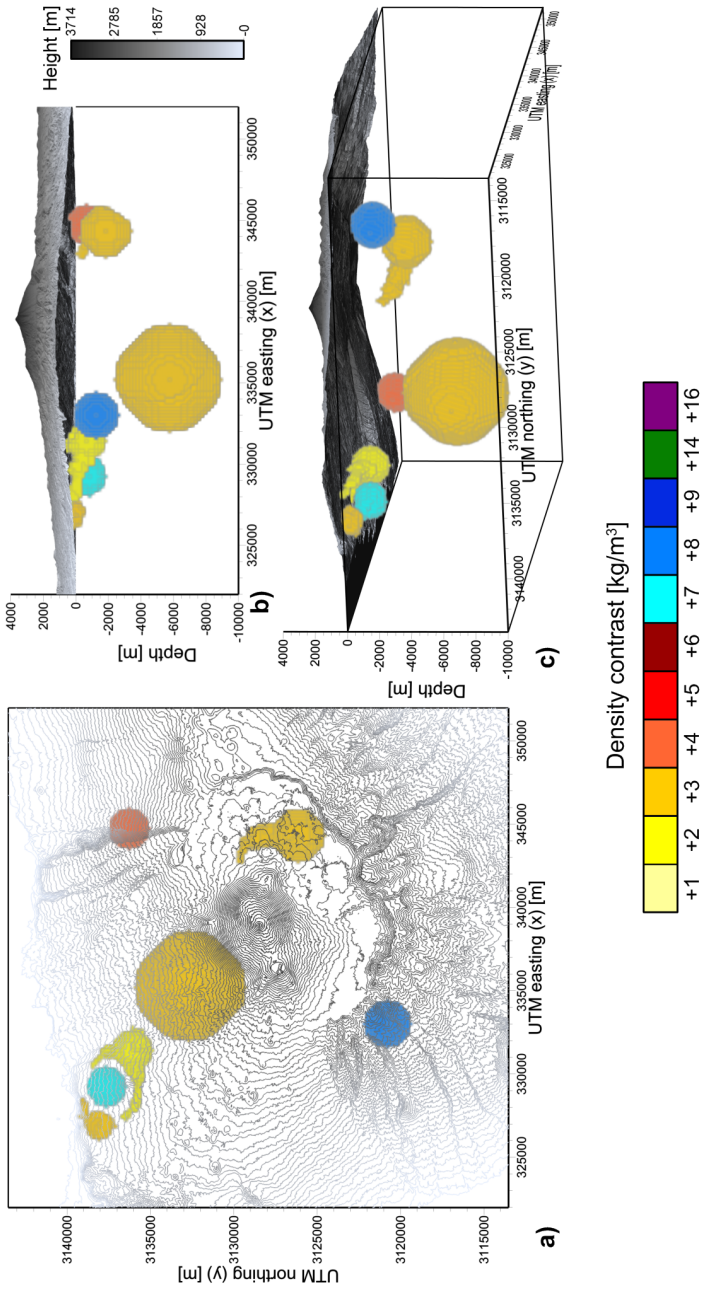


Fig. 10. Solution F. Source bodies with differential densities of +2, +3, +4, +7, and +8 kg/m³: (a) plan view, (b) and (c) are two different angle-views.

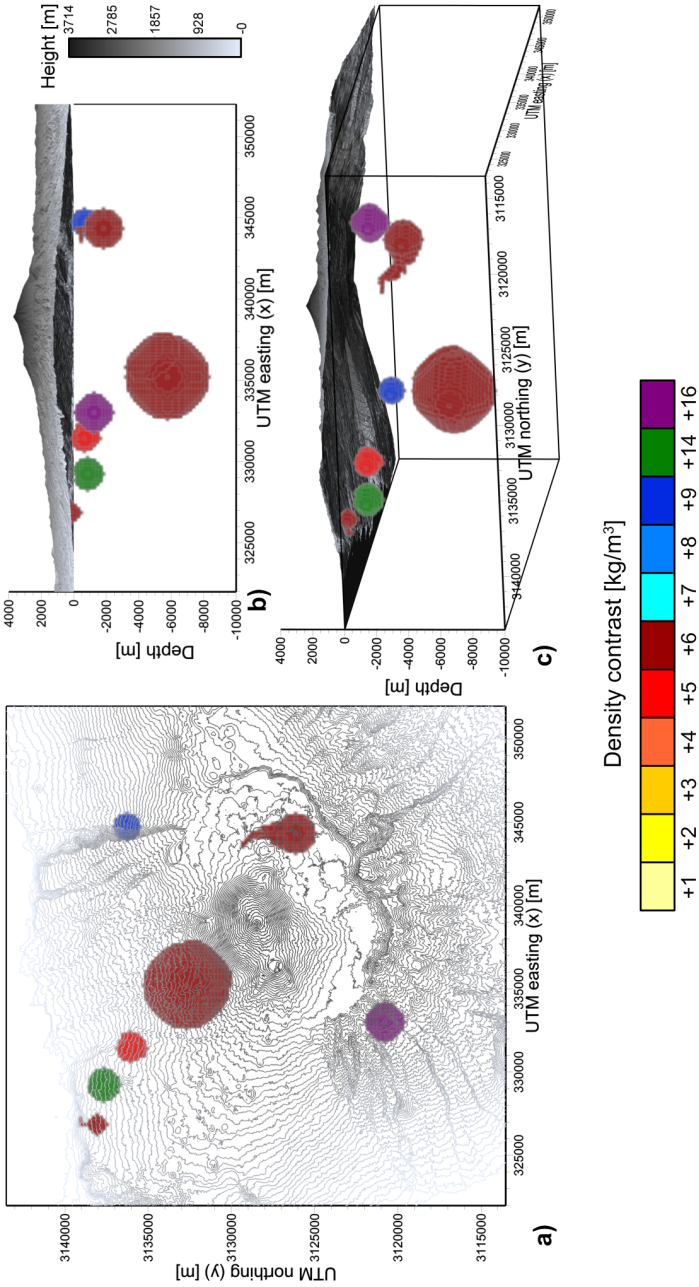


Fig. 11. Solution G. Source bodies with differential densities of +5, +6, +9, +14, and +16 kg/m³: (a) plan view, (b) and (c) are two different angle-views.

Table 2. Parameters of the source bodies of solution A shown in Fig. 5: $\delta\rho$ is differential density of the body, x and y are UTM easting and northing, z is height above sea level (of the center of the initial body seed), the next column lists the number of cells forming the body (which defines the volume of the body), m is the mass (time-lapse mass change) of the body and g is the amplitude (of the time-lapse change) of the surface gravity above the body. The last two columns are indicative of the contribution of the source body to the overall field. Notice that bodies grown from seeds 3, 6, and 7 (marked by *) merged in this solution into one body the parameters of which we list under body no. 3.

body	$\delta\rho$ [kg/m ³]	x (UTM) [m]	y (UTM) [m]	z [m]	number of cells	m [10 ⁹ kg]	g [μ Gal]
1	+1	332980	3120720	-1200	11621	92.968	55.866
2	+1	335180	3132720	-5800	39229	313.832	43.569
3	+1	329180	3137720	-800	* 7906	* 63.248	* 41.532
4	+1	344380	3126120	-1800	7469	59.752	24.570
5	+1	344780	3136320	-600	3492	27.936	23.911
6	+1	331380	3136120	-600	*	*	*
7	+1	326780	3138120	+200	*	*	*
8	-1	327180	3133920	-1000	4131	-33.048	-24.016
9	-1	338380	3119120	-800	4657	-37.256	-19.413
10	-1	334180	3140320	-4600	16107	-128.856	-15.197
11	-1	345780	3131720	-1000	6645	-53.160	-16.207

In Table 5 we list for each solution the number of iterations necessary for the calculation of the solution (the final solution is taken from the iteration with the smallest residual surface gravity) and the extremal values and rms of the residual surface gravity.

5. Discussion

As declared in the Introduction, our objective was to investigate the variability of the sizes and shapes of the source bodies (depending on the selection of their differential densities) obtained by the harmonic inversion from the time-lapse gravity changes observed in volcanic areas. We performed this analysis on temporal gravity changes accompanying the 2004–2005 unrest at the Central Volcanic Complex of Tenerife, Canary Islands. Here we do not

Table 3. Parameters of the source bodies of solution B shown in Fig. 6: $\delta\rho$ is differential density of the body, x and y are UTM easting and northing, z is height above sea level (of the center of the initial body seed), the next column lists the number of cells forming the body (which defines the volume of the body), m is the mass (time-lapse mass change) of the body and g is the amplitude (of the time-lapse change) of the surface gravity above the body. The last two columns are indicative of the contribution of the source body to the overall field.

body	$\delta\rho$ [kg/m ³]	x (UTM) [m]	y (UTM) [m]	z [m]	number of cells	m [10 ⁹ kg]	g [μ Gal]
1	+2	332980	3120720	-1200	5610	89.760	55.510
2	+1	335180	3132720	-5800	42088	336.704	44.674
3	+2	329180	3137720	-800	2347	37.552	33.342
4	+1	344380	3126120	-1800	6922	55.376	23.656
5	+1	344780	3136320	-600	3318	26.544	23.264
6	+1	331380	3136120	-600	2565	20.520	16.473
7	+1	326780	3138120	+200	843	6.744	12.905
8	-1	327180	3133920	-1000	4359	-34.872	-24.400
9	-1	338380	3119120	-800	6747	-53.976	-19.872
10	-1	334180	3140920	-4600	16901	-135.208	-15.765
11	-1	345780	3131720	-1000	6272	-50.176	-16.547

attempt to interpret the found solutions in terms of physical (volcanic) processes associated with magma and volatiles migration during volcanic unrest or reactivation. That is left for the next stage and future case studies employing constraints from other earth science disciplines and incorporating expertise of volcanologists.

In general, we can observe that for higher differential density values the source bodies grow from their initial quasi-spherical shape only slightly (or not at all), while retaining their shape. On the contrary, for smaller differential density values the bodies tend to grow more and acquire more complex shapes, sometimes displaying tentacles that may even mediate connections among the individual bodies (see e.g. Fig. 5), or the bodies may form contacts among each other. This feature – the tentacles – seems very intriguing. We have yet to determine whether the tentacles are an artefact – either of the iterative process (of the inversion procedure) or of the interpolation –

Table 4. Parameters of the source bodies of solution G shown in Fig. 11: $\delta\rho$ is differential density of the body, x and y are UTM easting and northing, z is height above sea level (of the center of the initial body seed), the next column lists the number of cells forming the body (which defines the volume of the body), m is the mass (time-lapse mass change) of the body and g is the amplitude (of the time-lapse change) of the surface gravity above the body. The last two columns are indicative of the contribution of the source body to the overall field.

body	$\delta\rho$ [kg/m ³]	x (UTM) [m]	y (UTM) [m]	z [m]	number of cells	m [10 ⁹ kg]	g [μ Gal]
1	+16	332980	3120720	-1200	689	88.192	61.425
2	+6	335180	3132720	-5800	8200	393.600	44.589
3	+14	329180	3137720	-800	417	46.704	40.971
4	+6	344380	3126120	-1800	951	45.648	21.754
5	+9	344780	3136320	-600	257	18.504	19.756
6	+5	331380	3136120	-600	324	12.960	13.178
7	+6	326780	3138120	+200	92	4.416	10.027
8	-8	327180	3133920	-1000	443	-28.352	-22.524
9	-6	338380	3119120	-800	443	-21.264	-19.495
10	-2	334180	3140120	-4600	14972	-239.552	-18.532
11	-4	345780	3131720	-1000	597	-19.104	-14.850

Table 5. Goodness of fit for the particular solutions (listed in the first column): number of iterations necessary for the calculation of the solution and the extremal values and rms of the residual surface gravity (i.e. the difference of the input gravity and calculated gravity; thus it is equal to negative misfit).

solution	number of iterations	min g [μ Gal]	max g [μ Gal]	rms g [μ Gal]
A	112	-3.079	1.260	0.538
B	136	-3.948	1.501	0.637
C	88	-4.332	1.844	0.820
D	8	-8.669	0.942	1.796
E	8	-10.716	2.143	1.908
F	208	-3.274	8.069	0.695
G	208	-4.659	8.688	1.003

or if they are realistic and indicate pathways of higher permeability for hydrothermal fluids or weakened zones yielding to diking or magma migration. The mass or gravity effect of the tentacles is smaller than those of the bodies, which could make us inclined towards the view that these tentacles are insignificant and hence artificial. On the other hand, they seem to mediate pathways among the bodies that appear meaningful. Moreover, one of the tentacles creeps towards the close vicinity of the Pico Viejo summit crater. Anyhow, the story of the presence of these tentacles is left for future investigations in terms of case studies where constraints from other geoscientific disciplines may help to resolve this issue.

The solutions with source bodies of smaller differential densities and more complex shapes manage to reach a better fit to the input gravity data than those with bodies of higher differential densities and smaller sizes with more spherical shapes (cf. Table 5). On the other hand, the bodies of such small differential density as 1 kg/m^3 might be unrealistically overgrown compared to real volcanic causes. How to approach their interpretation from this point of view shall be also the topic of future studies. One option is to view them as volumetric zones delineating the possible presence of magmatic/hydrothermal sources of higher differential densities and lesser dimensions discretely distributed within the zones (such as dike/sill swarms or magma patches). Additional studies are needed to handle this issue.

6. Conclusions

We studied here for the first time the performance of the harmonic inversion method when applied to time-lapse gravity changes in volcanic areas. This study, carried out on gravity changes observed during the 2004/5 volcanic unrest on Tenerife, was devoted to analyzing the variability of solutions with respect to the choice of free parameters of the methodology, first of all, the differential densities (temporal density changes) of the source bodies (volumetric domains of homogeneous density changes). We obtained several solutions for various combinations of the differential density values assigned to the individual source bodies and observed that the sizes of the bodies are in the inverse proportion to their differential densities (what can be expected theoretically). The variability of the solutions is the consequence of the non-uniqueness of the gravimetric inverse problem.

This case study gave us important experience with respect to the correct choice of several free parameters needed to initiate the iterative procedure (foremost the differential densities and radii of the seeds of the source bodies) and the method itself could be improved (see the end of chapter Harmonic inversion method).

In potential field inverse problems we often deal with composite signals while the decomposition into multiple sources inherently remains an ambiguous task. Due to the non-uniqueness of the inverse gravimetric problem also the solutions found by our harmonic inversion are again amongst many admissible solutions. Additional constraints from other earth science disciplines are required to validate physical (geologic, volcanologic) feasibility of any such solution. However, it is of great advantage when gravimetry alone provides several sets of admissible solutions that later on may be discriminated using available geologic or geoscientific constraints in the search for the most probable realistic scenario.

The case study based on the 2004/5 time-lapse gravity changes of the CVC on Tenerife indicates that the harmonic inversion methodology appears promising for inverting and interpreting gravity changes observed in volcanic areas during unrest or reactivation. In the follow-up work we shall attempt to assign volcanological interpretation to the source bodies presented here. Additional case studies, in general, are needed to establish the link between the solutions obtained by the harmonic inversion method and their physical interpretation in terms of processes taking place inside the volcano edifice or deeper below.

Acknowledgments. This work was supported by the Slovak Research and Development Agency under the contract No. APVV-0724-11 and by the Vega grant agency under grant projects No. 2/0042/15 and 1/0141/15.

References

- Brimich L., Fernández J., Granell R. D. R., Hvoždara M., 1996: Some comments on the effects of earth models on ground deformation modelling. *Studia Geophysica et Geodaetica*, **40**, 14–24.
- Brimich L., Charco M., Kohút I., Fernández J., 2011: 3D analytical and numerical modelling of the regional topography influence on the surface deformation due to underground heat source. *Contributions to Geophysics and Geodesy*, **41**, 3, 251–165.

-
- Charco M., Brimich L., Fernández J., 2002. Topography effects on the displacements and gravity changes due to magma intrusion. *Geologica Carpathica*, **53**, 4, 215–221.
- Gottsmann J., Wooller L., Martí J., Fernández J., Camacho A. G., Gonzalez P. J., Garcia A., Rymer H., 2006: New evidence for the reawakening of Teide volcano. *Geophys. Res. Lett.*, **33**, L20311, doi: 10.1029/2006GL027523.
- Pánisová J., Fraštia M., Wunderlich T., Pašteka R., Kušnirák D., 2013: Microgravity and Ground-penetrating Radar Investigations of Subsurface Features at the St Catherine's Monastery, Slovakia. *Archaeological Prospection*, **20**, 163–174, doi: 10.1002/arp.1450.
- Pohánka V., 2001: Application of the harmonic inversion method to the Kolárovo gravity anomaly, *Contributions to Geophysics and Geodesy*, **31**, 4, 603–620.
- Pohánka V., 2003a: The harmonic inversion method: calculation of the multi-domain density. *Contributions to Geophysics and Geodesy*, **33**, 4, 247–266.
- Pohánka V., 2003b: Testing of two variants of the harmonic inversion method on the territory of the eastern part of Slovakia. Geophysical Institute SAS, accessed 30 November 2015, <<http://gpi.savba.sk/GPIweb/ogg/pohanka/East1.ppt>>.
- Pohánka V., 2005: Universal interpolation method for many-dimensional spaces. Geophysical Institute SAS, accessed 30 November 2015, <<http://gpi.savba.sk/GPIweb/ogg/pohanka/int.pdf>>.